Inorganic Chemistry

Article

pubs.acs.org/IC

Synthesis and Characterization of Antiapicophilic Arsoranes and Related Compounds

Xin-Dong Jiang,*[†,‡] Shiro Matsukawa,[‡,§] Satoshi Kojima,[‡] and Yohsuke Yamamoto*[‡]

[†]The Key Laboratory for Special Functional Materials, Ministry of Education, Henan University, Kaifeng, 475-004, China

[‡]Department of Chemistry, Graduate School of Science, Hiroshima University,1-3-1 Kagamiyama, Higashi-Hiroshima, 739-8526, Japan

[§]Department of Chemistry, Faculty of Science, Toho University, 2-2-1 Miyama, Funabashi, 274-8510, Japan

Supporting Information

ABSTRACT: Utilizing bulky bidentate ligand systems with C_2F_5 and n-C_3F_7 groups, antiapicophilic arsoranes (**5b** and **5c**, respectively) were synthesized. A kinetic study on the isomerization of these arsoranes to their more stable isomers showed that the barriers increased in the order of CF_3 < C_2F_5 < n-C_3F_7 in accord with their steric bulk. It was also revealed that the degree of freezing isomerization was larger for the change from CF_3 to C_2F_5 than from C_2F_5 to n-C_3F_7, obvious from the differences in activation free energy at 363 K of 1.6 and 0.3 kcal mol^{-1}, respectively. X-ray structural analysis of several precursors of these two systems disclosed the unique structures of these compounds.

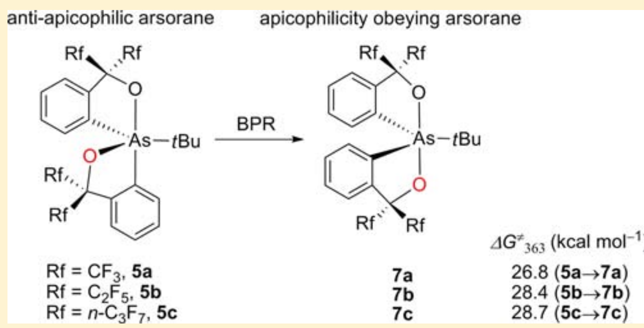

■ INTRODUCTION

Hypervalent compounds of the main group elements have been attracting increasing interest by both experimental and theoretical chemists for quite a while.[1] Especially of note is hypervalent phosphorus (phosphorane) chemistry,[2−5] due to its relevance to the phosphoryl transfer reaction in biological systems,[6−9] since formation or hydrolysis of biologically relevant phosphorus compounds[10−12] such as DNA or RNA involves hypervalent[13] 10-P-5[14−16] phosphorus as intermediates or transition states. Although hypervalent 10-As-5 arsenic compounds (arsoranes) have been investigated to a lesser extent, they are significant as intermediates in reactions of arsonium ylides with carbonyl compounds to form olefins or epoxides.[17−26] Thus, to clarify the mechanism of such reactions, comprehensive knowledge of the thermodynamic and kinetic properties of the transient species would be needed, and in turn, it is quite important to establish an understanding of the difference in structure and reactivity of isomeric pentacoordinate compounds.

Pentacoordinate compounds are known to adopt two different structures: one is a trigonal bipyramid (TBP) structure, and the other is a square pyramid (SP) structure, and the former is generally preferred. The TBP structure includes two distinct bonds: the apical bond and the equatorial bond. The apical bond is described as a three-center-four-electron (hypervalent) bond, whereas the equatorial bond is described as an sp^2 bond. The apical bond is comprised of two sites positioned linearly with the center intersecting with the equatorial plane perpendicularly. This structural characteristic brings about two unique features, i.e., apicophilicity[27−45] and facile stereomutation usually interpreted by the Berry pseudorotation (BPR) mechanism.[46] The former is the propensity for more electronegative and sterically less bulky groups to prefer the apical sites, and the latter is a low-energy nondissociative intramolecular site exchange process peculiar to TBP molecules. An alternative mechanism called turnstile rotation (TR) proposed by Ugi et al.[47−50] has been calculated to be higher in energy than BPR. Recently, Lammertsma proposed that TR can be explained as a special combination of BPRs.[51]

As for 10-P-5 compounds, using the Martin ligand (Figure 1, **A**),[13] we succeeded in freezing the BPR enough to isolate a series of phosphoranes violating the apicophilicity concept with an oxygen-equatorial carbon-apical configuration (O-equatorial).[52−60] These phosphoranes are kinetically stabilized products and can still be converted into their corresponding more stable stereoisomers with a carbon-equatorial oxygen-apical config-

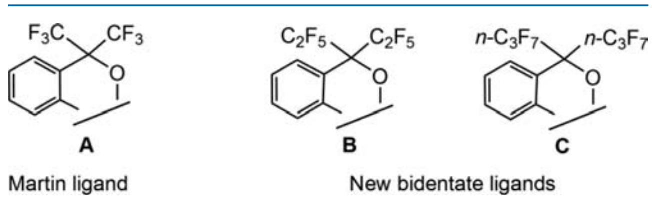

Figure 1. Reported bidentate ligands for freezing Berry pseudorotation used in the present study.

Received: July 11, 2012
Published: September 26, 2012

uration (O-apical). Furthermore, we recently developed a new bidentate ligand bearing two C_2F_5 groups (Figure 1, **B**), which was more effective for freezing the BPR of the phosphoranes than the Martin ligand.[23,61−67] More recently, we also developed an even more bulky bidentate ligand **C** bearing two n-C_3F_7 groups, which had a larger capability to freeze the BPR of phosphoranes (Figure 1, **C**).[68] However, unlike the situation with phosphorus chemistry, little is known about hypervalent arsenic species (arsoranes), one reason being that arsoranes often suffer from BPR faster than the corresponding phosphoranes.[69] For example, the activation free energy of Ph_2PF_3 at its coalescence temperature (379 K) was determined to be 18.7 kcal mol^{-1},[70] whereas the single fluorine signal of Ph_2AsF_3 observed at room temperature did not decoalesce even at −90 °C.[71] A theoretical study has shown the energy of BPR for AsF_5 (3.0 kcal mol^{-1}) to be lower than that of PF_5 (4.3 kcal mol^{-1}).[72] As we have done for the phosphoranes, investigation of each isolated stereoisomer of the arsoranes would lead to a better understanding of the general and fundamental properties of pentacoordinate arsoranes. Recently, we communicated our preliminary studies on 10-As-5 compounds with ligands **A** and **B**.[64] Herein, we systematically report on the synthesis of O-equatorial arsoranes and kinetic study of their pseudorotation to the more stable O-apical isomers with the three ligands **A**−**C**. In addition, the unique structures of a series of arsenic species, including O-equatorial arsoranes, O-apical arsoranes, an arsine, a tetracoordinate arsoranide, hydroxyarsoranes, and iodoarsoranes, determined by crystallography are presented.

■ EXPERIMENTAL SECTION

General Procedures. Melting points were measured using a Yanaco micromelting point apparatus and are uncorrected. ^{1}H NMR (400 MHz) and ^{19}F NMR (376 MHz) spectra were recorded using a JEOL EX-400 or a JEOL AL-400 spectrometer. ^{1}H NMR chemical shifts (δ) are given in ppm downfield from Me_4Si, determined by residual chloroform (δ = 7.26 ppm). ^{19}F NMR chemical shifts (δ) are given in ppm downfield from the external $CFCl_3$. Elemental analyses were performed using a Perkin-Elmer 2400 CHN elemental analyzer. All reactions were carried out under N_2. Tetrahydrofuran (THF) and diethyl ether (Et_2O) were freshly distilled from Na−benzophenone, n-hexane was distilled from Na, and other solvents were distilled from CaH_2. Merck silica gel 60 was used for column chromatography.

*2-[3,3-Bis(trifluoromethyl)-2,1-benzoxarsol-1(3H)-yl]-α,α-bis-(trifluoromethyl)benzenemethanol (**2a**).* Under N_2, TMEDA (1.60 mL, 10.6 mmol) was added to n-BuLi (1.58 M n-hexane solution, 14.0 mL, 22.1 mmol) at room temperature, and the mixture was stirred for 20 min. 1,1,1,3,3,3-Hexafluoro-2-phenyl-2-propanol (1.70 mL, 10.1 mmol) in THF (1.0 mL) was then added at 0 °C, and the mixture was stirred for 8 h at room temperature. The mixture was then transferred to a solution of $AsCl_3$ (0.42 mL, 5.0 mmol) in THF (5.0 mL) at −78 °C. The mixture was warmed to room temperature and stirred for 12 h. The reaction was quenched with distilled water (2 × 50 mL). The mixture was extracted with ether (2 × 80 mL) and dried over anhydrous $MgSO_4$. After removing the solvents by evaporation, the resulting crude mixture was subjected to recrystallization from n-hexane to afford **2a** (1.22 g, 2.18 mmol, 21%) as a white solid. Compound **4a−Li** (1.47 g, 2.61 mmol, 26%) was obtained as a colorless liquid from the filtrate. Colorless crystals of **2a·THF** suitable for X-ray analysis were obtained by further recrystallization from n-hexane. Unfortunately only small crystals of low quality inevitably containing THF could be obtained. However, the GOF value validates our assignments. **2a**: mp 148.0−149.0 °C (decomp.). ^{1}H NMR ($CDCl_3$): δ = 8.32 (br s, 1H), 8.04 (br s, 1H), 7.77 (br s, 1H), 7.61 (s, 2H), 7.47 (t, $^3J_{HH}$ = 7.6 Hz, 2H), 7.40 ppm (t, $^3J_{HH}$ = 7.6 Hz, 2H). ^{19}F NMR ($CDCl_3$): δ = −73.7 (q, $^4J_{FF}$ = 8.6 Hz, 3F), −73.9 (q, $^4J_{FF}$ = 8.6 Hz, 3F), −76.2 (q, $^4J_{FF}$ = 8.2 Hz, 3F), −77.2 ppm (q, $^4J_{FF}$ = 8.2 Hz, 3F). Anal. Calcd for $C_{20}H_{13}AsF_{12}O_{2.5}$ (**2a**·0.5THF): C, 40.29; H, 2.20. Found: C, 40.26; H, 2.10. **4a−Li**: mp 102.0−103.0 °C (decomp.). ^{1}H NMR ($CDCl_3$): δ = 8.06 (d, $^3J_{HH}$ = 7.6 Hz, 2H), 7.60 (d, $^3J_{HH}$ = 7.6 Hz, 2H), 7.39 (td, $^3J_{HH}$ = 7.6 Hz, $^4J_{HH}$ = 1.2 Hz, 2H), 7.32 ppm (td, $^3J_{HH}$ = 7.6 Hz, $^4J_{HH}$ = 1.2 Hz, 2H). ^{19}F NMR ($CDCl_3$): δ = −73.8 (q, $^4J_{FF}$ = 8.6 Hz, 6F), −76.3 ppm (q, $^4J_{FF}$ = 8.6 Hz, 6F).

*[TBPY-5-12]-1-(1,1-dimethylethyl)-3,3,3′,3′-tetrakis-(trifluoromethyl)-1λ^5-1,1′(3H,3′H)-spirobi[2,1-benzoxarsole] (**5a**).* Under N_2, t-BuLi (1.57 M n-pentane solution, 0.35 mL, 0.549 mmol) was added to a solution of **2a** (101 mg, 0.181 mmol) in Et_2O (3.0 mL) at −78 °C. The mixture was then stirred for 1 h at room temperature. I_2 (139 mg, 0.549 mmol) was added at −78 °C, and the mixture was stirred for 1 h at 0 °C. The reaction was quenched with aqueous $Na_2S_2O_3$ (2 × 20 mL). The mixture was extracted with Et_2O (2 × 50 mL), and the organic layer was washed with brine (2 × 30 mL) and dried over anhydrous $MgSO_4$. After removing the solvents by evaporation, the resulting crude mixture was separated by preparative TLC (n-hexane:CH_2Cl_2 = 4:1) to afford **5a** (56.5 mg, 0.0916 mmol, 50%) and **3a** (21.5 mg, 0.0373 mmol, 21%) as white solids. Colorless crystals of **5a** and **3a** suitable for X-ray analysis were obtained by recrystallization from n-hexane/CH_2Cl_2. **5a**: mp 130.0−130.8 °C (decomp.). ^{1}H NMR ($CDCl_3$): δ = 7.92 (br d, $^3J_{HH}$ = 6.8 Hz, 2H), 7.84 (br d, $^3J_{HH}$ = 6.8 H, 2H), 7.60−7.67 (m, 4 H), 1.39 ppm (s, 9H). ^{19}F NMR ($CDCl_3$): δ = −73.6 (q, $^4J_{FF}$ = 8.6 Hz, 6F), −76.3 ppm (q, $^4J_{FF}$ = 8.6 Hz, 6F). Anal. Calcd for $C_{22}H_{17}AsF_{12}O_2$: C, 42.88; H, 2.78. Found: C, 42.68; H, 2.38. **3a**: mp 138.2−139.0 °C. ^{1}H NMR ($CDCl_3$): δ = 8.36 (d, $^3J_{HH}$ = 7.2 Hz, 2H), 7.91 (br d, $^3J_{HH}$ = 7.2 Hz, 2H), 7.82 (td, $^3J_{HH}$ = 7.2 Hz, $^4J_{HH}$ = 1.4 Hz, 2H), 7.77 (td, $^3J_{HH}$ = 7.2 Hz, $^4J_{HH}$ = 1.4 Hz, 2H), 3.33 ppm (s, 1H). ^{19}F NMR ($CDCl_3$): δ = −73.8 (q, $^4J_{FF}$ = 8.6 Hz, 6F), −74.4 ppm (q, $^4J_{FF}$ = 8.6 Hz, 6F). Anal. Calcd for $C_{18}H_9AsF_{12}O_3$: C, 37.52; H, 1.57. Found: C, 37.38; H, 1.30.

*2-[3,3-Bis(1,1,2,2,2-pentafluoroethyl)-2,1-benzoxarsol-1(3H)-yl]-α,α-bis(1,1,2,2,2-pentafluoroethyl)benzenemethanol (**2b**).* Under N_2, 1,1,1,2,2,4,4,5,5,5-decafluoro-3-(2-bromophenyl)-3-pentanol (934 mg, 2.21 mmol) was added to a slurry of NaH (199 mg, 4.97 mmol) in THF (3.0 mL) at 0 °C, and the mixture was stirred for 0.5 h at room temperature. To the mixture cooled to −78 °C, t-BuLi (1.57 M n-pentane solution, 2.90 mL, 4.55 mmol) was added, and the mixture was stirred for 1 h at the same temperature. The mixture was then transferred to a solution of $AsCl_3$ (0.095 mL, 0.113 mmol) in THF (3.0 mL) at −78 °C. The mixture was allowed to warm to room temperature and stirred for 18 h. The reaction was quenched with distilled water (2 × 50 mL). The mixture was extracted with ether (2 × 60 mL) and dried over anhydrous $MgSO_4$. After removing the solvents by evaporation, the resulting crude mixture was separated by column chromatography (n-hexane:CH_2Cl_2 = 5:1) to afford **2b** (215 mg, 0.384 mmol, 17%) containing 7% of hydroxyarsorane **3b** and **4b−Na** (278.8 mg, 0.408 mmol, 18%) as white solids. Colorless crystals of **3b** suitable for X-ray analysis were obtained by recrystallization of the mixture from n-hexane/CH_2Cl_2. Colorless crystals of **4b−Na MeOH·3H$_2$O** suitable for X-ray analysis were obtained by dissolving the solid in n-hexane at −17 °C and adding a few drops of MeOH to induce crystallization. Compound **2b** was gradually oxidized in air to give **3b**; therefore, **2b** was used in the following reaction without further purification. Similarly, compound **4b−Na** was oxidized in the open air to slowly give **3b**. **2b**: ^{1}H NMR ($CDCl_3$): δ = 8.19 (d, $^3J_{HH}$ = 7.8 Hz, 2H), 7.57 (br d, $^3J_{HH}$ = 7.8 Hz, 2H), 7.34 (td, $^3J_{HH}$ = 7.8 Hz, $^4J_{HH}$ = 1.2 Hz, 2H), 7.26 ppm (td, $^3J_{HH}$ = 7.8 Hz, $^4J_{HH}$ = 1.2 Hz, 2H). ^{19}F NMR ($CDCl_3$): δ = −78.1 (t, $^3J_{FF}$ = 18.5 Hz, 6F), −78.22 (s, 3F), −78.23 (s, 3F), −114.8 (s, 2F), −114.9 (s, 2F), −116.1 (dq, $^2J_{F-F}$ = 282 Hz, $^3J_{FF}$ = 18.5 Hz, 2F), −119.3 ppm (dq, $^2J_{FF}$ = 282 Hz, $^4J_{FF}$ = 18.5 Hz, 2F). **3b**: mp 112.1−113.0 °C. ^{1}H NMR ($CDCl_3$): δ = 8.48−8.46 (m, 2H), 7.90 (br s, 2H), 7.82−7.76 (m, 4H), 3.19 ppm (s, 1H). ^{19}F NMR ($CDCl_3$): δ = −78.3 (s, 6F), −78.8 (s, 6F), −115.5 (dm, $^2J_{FF}$ = 285 Hz, 2F), −117.2 to −117.3 (m, 4F), −120.0 ppm (dm, $^2J_{FF}$ = 285 Hz, 2F). Anal. Calcd for $C_{22}H_9AsF_{20}O_3$: C, 34.04; H, 1.17. Found: C, 33.89; H, 0.81. **4b−Na**: mp 109.1−109.9 °C (decomp.). ^{1}H NMR ($CDCl_3$): δ = 8.05 (d, $^3J_{HH}$ = 7.6 Hz, 2H), 7.60 (d, $^3J_{HH}$ = 7.6 Hz, 2H), 7.38 (td, $^3J_{HH}$ = 7.6 Hz, $^4J_{HH}$ = 1.2 Hz, 2H), 7.32 ppm (td, $^3J_{HH}$ = 7.6

Hz, $^4J_{HH}$ = 1.2 Hz, 2H). ^{19}F NMR ($CDCl_3$): δ = −78.2 (s, 6F), −78.6 (s, 6F), −115.0 (s, 4F), −118.0 (dm, $^2J_{FF}$ = 285.0 Hz, 2F), −120.0 ppm (dm, $^2J_{FF}$ = 285.0 Hz, 2F).

*[TBPY-5-12]-1-(1,1-dimethylethyl)-3,3,3′,3′-tetrakis(1,1,2,2,2-pentafluoroethyl)-1λ^5-1,1′(3H,3′H)-spirobi[2,1-benzoxarsole] (**5b**).* Under N_2, *t*-BuLi (1.57 M *n*-pentane solution, 0.30 mL, 0.471 mmol) was added to a solution of **2b** (113 mg, 0.142 mmol) in Et_2O (3.0 mL) at −78 °C. The mixture was then stirred for 1 h at room temperature. I_2 (115 mg, 0.452 mmol) was added at −78 °C, and the mixture was stirred for 1 h at 0 °C. The reaction was quenched with aqueous $Na_2S_2O_3$ (2 × 10 mL). The mixture was extracted with Et_2O (2 × 40 mL), and the organic layer was washed with brine (2 × 30 mL) and dried over anhydrous $MgSO_4$. After removing the solvents by evaporation, the resulting crude mixture was separated by preparative TLC (*n*-hexane:CH_2Cl_2 = 4:1) to afford **5b** (23.4 mg, 0.0287 mmol, 20%) as a white solid, followed by reversed-phase HPLC (MeCN) to afford **3b** (R_T = 20 min: 7.7 mg, 0.0099 mmol, 7%) and **6b** (R_T = 31.6 min: 19.2 mg, 0.0217 mmol, 15%) as white solids. Colorless crystals of **5b** and **6b** suitable for X-ray analysis were obtained by recrystallization from *n*-hexane/CH_2Cl_2. **5b**: mp 148.3−149.1 °C (decomp.). ^{1}H NMR ($CDCl_3$): δ = 7.98−7.96 (m, 2H), 7.81 (br d, $^3J_{HH}$ = 6.8 H, 2H), 7.63−7.61 (m, 4H), 1.35 ppm (s, 9H). ^{19}F NMR ($CDCl_3$): δ = −78.4 (s, 6F), −78.5 (s, 6F), −113.1 (s, 4F), −114.2 (d, $^2J_{FF}$ = 286 Hz, 2F), −115.9 ppm (d, $^2J_{FF}$ = 286 Hz, 2F). Anal. Calcd for $C_{26}H_{17}AsF_{20}O_2$: C, 38.26; H, 2.10. Found: C, 38.34; H, 2.07. **6b**: mp 155.0−155.5 °C. ^{1}H NMR ($CDCl_3$): δ = 8.49 (d, $^3J_{HH}$ = 5.6 Hz, 2H), 7.91 (br d, $^3J_{HH}$ = 5.6 Hz, 2H), 7.79 (td, $^3J_{HH}$ = 5.6 Hz, $^4J_{HH}$ = 1.5 Hz, 2H), 7.75 ppm (td, $^3J_{HH}$ = 5.6 Hz, $^4J_{HH}$ = 1.5 Hz, 2H). ^{19}F NMR ($CDCl_3$): δ = −78.4 (s, 6F), −78.8 (t, $^3J_{FF}$ = 19.5 Hz, 6F), −112.4 (d, $^2J_{FF}$ = 287.9 Hz, 2F), −115.6 (dq, $^2J_{FF}$ = 287.9 Hz, $^3J_{FF}$ = 19.5 Hz, 2F), −116.0 (dq, $^2J_{FF}$ = 287.9 Hz, $^3J_{FF}$ = 19.5 Hz, 2F), −120.4 ppm (d, $^2J_{FF}$ = 287.9 Hz, 2F). Anal. Calcd for $C_{22}H_8AsF_{20}IO_3$: C, 29.82; H, 0.91. Found: C, 29.88; H, 0.67.

*2-[3,3-Bis(1,1,2,2,3,3,3-heptafluoropropyl)-2,1-benzoxarsol-1(3H)-yl]-α,α-bis(1,1,2,2,3,3,3-heptafluoropropyl)benzenemethanol (**2c**).* Under N_2, 1,1,1,2,2,3,3,5,5,6,6,7,7,7-tetradecafluoro-4- (2-bromophenyl)-4-heptanol (1.78 g, 3.40 mmol) was added to a slurry of NaH (340.8 mg, 8.52 mmol) in THF (5.0 mL) at 0 °C, and the mixture was stirred for 0.5 h at room temperature. To the mixture cooled to −78 °C, *t*-BuLi (1.57 M *n*-pentane solution, 4.60 mL, 7.22 mmol) was added, and the mixture was stirred for 1 h at the same temperature. The mixture was then transferred to a solution of $AsCl_3$ (0.145 mL, 0.172 mmol) in THF (5.0 mL) at −78 °C. The mixture was allowed to warm to room temperature and stirred for 12 h. The reaction was quenched with distilled water (2 × 80 mL). The mixture was extracted with ether (2 × 100 mL) and dried over anhydrous $MgSO_4$. After removing the solvents by evaporation, the resulting crude mixture was subjected to recrystallization from *n*-hexane to afford a mixture of three compounds (**2c**:**3c**:**4c−Na** = 22:51:27 by ^{1}H and ^{19}F NMR). The mixture was then subjected to recrystallization from *n*-hexane/CH_2Cl_2 to afford **3c** (0.624 g, 0.64 mmol, 19%) as a white solid. Colorless crystals of **3c** suitable for X-ray analysis were obtained by further recrystallization from *n*-hexane/CH_2Cl_2. **3c**: mp 110.0−111.0 °C (decomp.). ^{1}H NMR ($CDCl_3$): δ = 8.45 (d, $^3J_{HH}$ = 7.2 Hz, 2H), 7.92 (br d, $^3J_{HH}$ = 7.2 Hz, 2H), 7.02 (td, $^3J_{HH}$ = 7.2 Hz, $^4J_{HH}$ = 1.5 Hz, 2H), 7.76 (td, $^3J_{HH}$ = 7.2 Hz, $^4J_{HH}$ = 1.5 Hz, 2H), 3.21 ppm (s, 1H). ^{19}F NMR ($CDCl_3$): δ = −80.9 (s, 6F), −81.4 (s, 6F), −111.2 (d, $^2J_{FF}$ = 291.6 Hz, 2F), −112.1 (d, $^2J_{FF}$ = 291.6 Hz, 2F), −114.4 (d, $^2J_{FF}$ = 291.6 Hz, 2F), −115.2 (d, $^2J_{FF}$ = 291.6 Hz, 2F), −120.2 (d, $^2J_{FF}$ = 291.6 Hz, 2F), −123.1 (d, $^2J_{FF}$ = 291.6 Hz, 2F), −124.1 (d, $^2J_{FF}$ = 291.6 Hz, 2F), −125.6 ppm (d, $^2J_{FF}$ = 291.6 Hz, 2F). Anal. Calcd for $C_{26}H_9AsF_{28}O_2$: C, 31.99; H, 0.93. Found: C, 31.73; H, 1.20.

*[TBPY-5-12]-1-(1,1-dimethylethyl)-3,3,3′,3′-tetrakis(1,1,2,2,3,3,3-heptafluoroproyl)-1λ^5-1,1′(3H,3′H)-spirobi[2,1-benzoxarsole] (**5c**).* Under N_2, *t*-BuLi (1.57 M *n*-pentane solution, 0.60 mL, 0.471 mmol) was added to a solution of **2c** (286.7 mg, 0.298 mmol) in Et_2O (5.0 mL) at −78 °C. The mixture was then stirred for 1 h at room temperature. I_2 (218.6 mg, 0.861 mmol) was added at −78 °C, and the mixture was stirred for 1 h at room temperature. The reaction was quenched with aqueous $Na_2S_2O_3$ (2 × 60 mL). The mixture was extracted with Et_2O (2 × 50 mL), and the organic layer was washed with brine (2 × 50 mL) and dried over anhydrous $MgSO_4$. After removing the solvents by evaporation, the resulting crude mixture was separated by preparative TLC (*n*-hexane:CH_2Cl_2 = 4:1) to afford **5c** (15.8 mg, 0.0155 mmol, 5%), **3c** (50.3 mg, 0.0512 mmol, 17%), and **6c** (48.8 mg, 0.0449 mmol, 15%) as white solids and **1c−H$_2$** (34.2 mg, 0.0769 mmol, 26%) as a colorless liquid. Colorless crystals of **5c** and **6c** suitable for X-ray analysis were obtained by recrystallization from *n*-hexane/CH_2Cl_2. Unfortunately crystals of good quality could not be obtained for **5c**, and the *R* value was somewhat high. However, the GOF value validates our assignments. **5c**: mp 114.0−115.0 °C (decomp.). ^{1}H NMR ($CDCl_3$): δ = 7.99−7.97 (m, 2H), 7.83 (br s, 2H), 7.63−7.61 (m, 4H), 1.34 ppm (s, 9H). ^{19}F NMR ($CDCl_3$): δ = −81.2 (t, $^3J_{FF}$ = 12.3 Hz, 6F), −81.5 (s, 6F), −109.0 (s, 4F), −111.6 (s, 4F), −120.4 (dq, $^2J_{FF}$ = 289.5 Hz, $^3J_{FF}$ = 12.3 Hz, 2F), −122.3 (dq, $^2J_{FF}$ = 289.5 Hz, $^3J_{FF}$ = 12.3 Hz, 2F), −123.8 (d, $^2J_{FF}$ = 289.5 Hz, 2F), −127.1 ppm (d, $^2J_{FF}$ = 289.5 Hz, 2F). Anal. Calcd for $C_{30}H_{17}AsF_{28}O_2$: C, 35.45; H, 1.69. Found: C, 35.40; H, 1.44. **6c**: mp 97.0−98.0 °C (decomp.). ^{1}H NMR ($CDCl_3$): δ = 8.49−8.46 (m, 2H), 7.85 (br s, 2H), 7.74−7.44 ppm (m, 4H). ^{19}F NMR ($CDCl_3$): δ = −80.9 (s, 6F), −81.5 (s, 6F), −110.5 (s, 4F), −111.3 (d, $^2J_{FF}$ = 288.3 Hz, 2F), −114.6 (d, $^2J_{FF}$ = 288.3 Hz, 2F), −119.8 (d, $^2J_{FF}$ = 288.3 Hz, 2F), −123.0, (d, $^2J_{FF}$ = 288.3 Hz, 2F), −124.6 (dm, $^2J_{FF}$ = 288.3 Hz, 2F), −125.9 ppm (dm, $^2J_{FF}$ = 288.3 Hz, 2F). Spectral data of **3c** were consistent with those of the same product obtained as the product described above. Spectral data for **1c−H$_2$** were consistent with those described in our reported paper.[68]

*[TBPY-5-12]-1-(1,1-dimethylethyl)-3,3′,3′-tetrakis(1,1,2,2,3,3,3-heptafluoroproyl)-1λ^5-1,1′(3H,3′H)-spirobi[2,1-benzoxarsole] (**7c**).* A solution of **5c** (14.2 mg, 0. 0139 mmol) in toluene (3.0 mL) was heated at 105 °C for 12 h. After concentration in vacuo, the residue was separated by column chromatography (*n*-hexane:CH_2Cl_2 = 4:1) to afford **7c** (14.0 mg, 0.0137 mmol, 98%) as a white solid. Colorless crystals of **7c** suitable for X-ray analysis were obtained by recrystallization from *n*-hexane/CH_2Cl_2. **7c**: ^{1}H NMR ($CDCl_3$): δ = 8.39−8.37 (m, 2H), 7.78 (br s, 2H), 7.65−7.62 (m, 4H), 1.29 ppm (s, 9H). ^{19}F NMR ($CDCl_3$): δ = −81.2 (s, 6F), −81.5 (s, 6F), −108.9 (br d, $^2J_{FF}$ = 293.2 Hz, 2F), −109.9 (br d, $^2J_{FF}$ = 293.2 Hz, 2F), −110.7 (d, $^2J_{FF}$ = 293.2 Hz, 2F), −112.7 (d, $^2J_{FF}$ = 293.2 Hz, 4F), −123.1 (d, $^2J_{FF}$ = 293.2 Hz, 4F), −124.6 ppm (d, $^2J_{FF}$ = 293.2 Hz, 2F). Anal. Calcd for $C_{30}H_{17}AsF_{28}O_2$: C, 35.45; H, 1.69. Found: C, 35.36; H, 1.64.

X-ray Crystal Structure Determinations of Arsenic Compounds. Crystals suitable for X-ray structural determination were mounted on a Mac Science DIP2030 imaging plate diffractometer and irradiated with graphite-monochromated Mo Kα radiation (λ = 0.71073 Å) for data collection. Unit cell parameters were determined by separately autoindexing several images in each data set using the DENZO program (MAC Science).[73] For each data set, the rotation images were collected in 3° increments with a total rotation of 180° about the φ axis. Data were processed using SCALEPACK. Structures were solved by a direct method with the SHELX-97 program.[74] Refinement on F^2 was carried out using full-matrix least-squares by the SHELX-97 program.[74] All non-hydrogen atoms were refined using the anisotropic thermal parameters. Hydrogen atoms were included in the refinement along with the isotropic thermal parameters. Crystal data and structure refinements of these arsenic species are listed in Tables 1−4.

■ RESULTS AND DISCUSSION

Synthesis of Arsines. Arsines **2**, along with hydroxyarsoranes **3** and arsoranides **4**, were prepared by treatment of $AsCl_3$ with 2-fold amounts of the corresponding bidentate ligands **1** (Scheme 1).[75] Compound **2a** showed four distinct fluorine signals corresponding to the CF_3 groups in the ^{19}F NMR spectrum (δ = −73.7, −73.9, −76.2, and −77.2 ppm at 25 °C), and the two aromatic rings were equivalently observed by ^{1}H NMR. This indicates that compound **2a** is a trivalent arsine in the solution state, and it is in clear contrast to the phosphorus

Table 1. Crystal and Refinement Data for 2a·THF, 3a, and 3b

	2a·THF	3a	3b
formula	$C_{22}H_{17}AsF_{12}O_3$	$C_{18}H_9AsF_{12}O_3$	$C_{22}H_9AsF_{20}O_3$
M_w	632.27	576.17	776.21
cryst syst	triclinic	triclinic	monoclinic
space group	*P*-1	*P*-1	$P2_1/c$
color	colorless	colorless	colorless
habit	plate	plate	plate
a, Å	8.7080(8)	11.5340(2)	13.4940(4)
b, Å	10.9580(10)	12.6580(2)	8.2620(2)
c, Å	13.7650(4)	15.0050(2)	23.4950(7)
α, deg	75.472(3)	67.2910(10)	90
β, deg	76.821(4)	87.6990(10)	97.2910(1)
γ, deg	73.579(10)	88.6520(10)	90
V, Å^3	1202.0(2)	2019.16(5)	2598.22(13)
Z	2	4	4
D_{calcd}, g cm^{-3}	1.747	1.895	1.984
abs. coeff., mm^{-1}	1.531	1.812	1.479
F(000)	628	1128	1512
radiation, *λ*, Å	Mo K*α*, 0.71073	Mo K*α*, 0.71073	Mo K*α*, 0.71073
T, K	293(2)	293(2)	298(2)
data, collected	+*h*, ± *k*, ± *l*	+*h*, ± *k*, ± *l*	+*h*, +*k*, ± *l*
data/restraints/ params	3866/0/344	8827/0/615	5610/0/416
R_1 [$I > 2\sigma(I)$]	0.1832	0.0455	0.0471
wR_2 (all data)	0.4798	0.1309	0.1394
GOF	1.093	1.086	1.143
CCDC No.	886009	886010	886011

Table 2. Crystal and Refinement Data for 3c, 4b−Na·MeOH·3H$_2$O, and 5a

	3c	4b−Na·MeOH·3H$_2$O	5a
formula	$C_{26}H_9AsF_{28}O_3$	$C_{23}H_{18}AsF_{20}O_6Na$	$C_{22}H_{17}AsF_{12}O_2$
M_w	976.25	868.28	616.28
cryst syst	triclinic	monoclinic	monoclinic
space group	*P*-1	$P2_1/c$	$P2_1/c$
color	colorless	colorless	colorless
habit	plate	plate	plate
a, Å	9.8340(2)	10.5860(2)	8.3040(3)
b, Å	12.6640(3)	27.3010(6)	16.0250(7)
c, Å	13.9860(2)	11.1630(3)	17.9010(10)
α, deg	75.133(2)	90	90
β, deg	69.4430(10)	109.3920(10)	99.950(2)
γ, deg	77.5720(10)	90	90
V, Å^3	1561.14(5)	3043.17(12)	2346.28(19)
Z	2	4	4
D_{calcd}, g cm^{-3}	2.077	1.895	1.745
abs. coeff., mm^{-1}	1.289	1.293	1.563
F(000)	948	1712	1224
radiation, *λ*, Å	Mo K*α*, 0.71073	Mo K*α*, 0.71073	Mo K*α*, 0.71073
T, K	173(2)	173(2)	173(2)
data, collected	+*h*, ± *k*, ± *l*	+*h*, +*k*, ± *l*	+*h*, +*k*, ± *l*
data/restraints/ params	6884/0/524	6079/0/462	4781/0/337
R_1 [$I > 2\sigma(I)$]	0.0521	0.0467	0.0508
wR_2 (all data)	0.1519	0.1517	0.1425
GOF	1.069	1.120	1.145
CCDC No.	886012	886013	639282

analogue which exists as a pentacoordinate hydrophosphorane with an equatorial P−H bond.[76,77] Although **2a** was stable to air, **2b** and **2c** were gradually oxidized in the open air to give the corresponding hydroxyarsoranes **3b** and **3c**, respectively. The arsoranides **4** were easily separated from **2** by recrystallization (*n*-hexane) or TLC (*n*-hexane/CH_2Cl_2).[67] Compound **4a-Li** bearing the Martin ligand (**A**) was very stable to water or air,[75] but **4b−Na** and **4c−Na** showed instability and slowly gave **3b** and **3c**, respectively.

Structure of Arsenic Species. The unique trivalent structure of **2a·THF** was confirmed by X-ray crystallography (Figure 2), in which the interatomic distances As1···O1 and As1−O2 of **2a THF** were 2.465 and 1.890 Å, respectively. The As1···O1 distance was significantly shorter than the sum of the van der Waals radii for arsenic and oxygen (3.37 Å) by 0.91 Å,[78] suggesting that there is interaction between As1 and O1. Hydroxyarsorane **3a** was obtained as one of the byproducts in the following synthesis of the O-equatorial arsorane **5a**. The ORTEP diagrams for **3a**, **3b**, and **3c** are shown in Figure 3. Selected bond lengths and angles are summarized in Table 5. The apical bond angles O1−As1−O2 of **3** (179.03(9)° for **3a**, 179.20(10)° for **3b**, and 178.12(9)° for **3c**) are nearly of the ideal value of 180°, and the sums of the equatorial angles (C1−As1−C2, C2−As1−O3, and O3−As1−C1) for **3a**, **3b**, and **3c** are 360°, 360°, and 359.99°, respectively, thus indicating that one of the byproduct compounds **3** with a hydroxyl group as a monodentate ligand at the equatorial site takes on nearly ideal trigonal-bipyramidal (TBP) structures. Colorless crystals for **4b−Na·MeOH·3H$_2$O** suitable for X-ray crystallography were obtained by dissolving the solid in *n*-hexane and adding a few drops of methanol to induce crystallization, Figure 4. Selected bond lengths and angles are summarized in Table 6. The C1−As1−C2 angle of **4b−Na·MeOH·3H$_2$O** (107.37°) is expanded by 6.5° compared with that of the CF_3 analog **4a−Et$_4$N** (100.9°) reported by our group.[75] This is in good agreement with the trend observed for analogous 10-Sb-4 compounds in which the corresponding angles are 110.3° for the C_2F_5 derivative[67] and 103.6° for the CF_3 derivative.[66] This should be due to steric repulsion between the *endo*-C_2F_5 group and the equatorial aromatic ring of the other bidentate. Other structural parameters for **4a−Et$_4$N** and **4b−Na MeOH·3H$_2$O** around the arsenic atom were very similar. The O1−As1−O2 angles of **4b−Na·MeOH·3H$_2$O** and **4a−Et$_4$N** are 168.39° and 169.0°, respectively, and thus distorted from the ideal value of 180° to some extent. Analysis of the *D* angles (61.01° and 68.1°, respectively) according to the method of Seppelt indicate that the structures should be classified as trigonal bipyramids and not square pyramids.[79]

Synthesis of the O-Equatorial Arsoranes. In order to prepare antiapicophilic arsoranes, we chose the *tert*-butyl group as the monodentate ligand since it was the most effective ligand for slowing isomerization of the series of O-equatorial phosphoranes to their corresponding O-apical isomers.[52,53] The antiapicophilic arsoranes **5** could then be synthesized from the corresponding arsines **2**, utilizing our reported method for synthesis of O-equatorial spirophosphoranes using I_2 as the oxidizing agent (Scheme 2).[53] Byproducts in the reactions were hydroxyarsoranes **3**, iodoarsoranes **6** (**6b** and **6c**), and the protonated bidentate ligand **1c−H$_2$**.[68] Interestingly, the iodoarsoranes **6** were stable enough to bear aqueous workup and chromatographic treatment. These are rare examples of water-stable iodoarsoranes. In contrast, for the CF_3 system **6a** was not obtained, suggesting that it is highly unstable to water.

Table 3. Crystal and Refinement Data for 5b, 5c, 6b, and 6c

	5b	5c	6b	6c
formula	$C_{26}H_{17}AsF_{20}O_2$	$C_{30}H_{17}AsF_{28}O_2$	$C_{22}H_8AsF_{20}IO_2$	$C_{26}H_8AsF_{28}IO_2$
M_w	816.32	1016.36	886.10	1086.14
cryst syst	monoclinic	triclinic	orthorhombic	monoclinic
space group	$P2_1/c$	*P*-1	*Pbcn*	*C*2/*c*
color	colorless	colorless	colorless	colorless
habit	plate	plate	plate	plate
a, Å	12.714(2)	9.4410(2)	18.5530(4)	22.9310(4)
b, Å	13.013(2)	10.7300(3)	8.8470(2)	15.0300(3)
c, Å	18.608(2)	18.2820(6)	16.8740(2)	9.6610(3)
α, deg	90	105.0530(10)	90	90
β, deg	109.1290(10)	100.9890(10)	90	100.717(1)
γ, deg	90	94.4480(10)	90	90
V, Å^3	2908.6(7)	1739.82(8)	2769.67(9)	3271.61(13)
Z	4	2	4	4
D_{calcd}, g cm^{-3}	1.864	1.940	2.125	2.205
abs. coeff., mm^{-1}	1.324	1.159	2.499	2.172
F(000)	1608	996	1688	2072
radiation, λ, Å	Mo Kα, 0.71073	Mo Kα, 0.71073	Mo Kα, 0.71073	Mo Kα, 0.71073
T, K	173(2)	173(2)	298(2)	200(2)
data, collected	+*h*, +*k*, ± *l*	+*h*, ± *k*, ± *l*	+*h*, ± *k*, ± *l*	+*h*, +*k*, ± *l*
data/restraints/params	6597/0/437	7701/0/555	3203/0/218	3755/0/264
R_1 [$I > 2\sigma(I)$]	0.0605	0.1153	0.0559	0.0413
wR_2 (all data)	0.1706	0.3577	0.2138	0.1326
GOF	1.071	1.135	1.121	1.257
CCDC No.	639283	886014	886015	886016

Table 4. Crystal and Refinement Data for 7a, 7b, and 7c

	7a	7b	7c
formula	$C_{22}H_{17}AsF_{12}O_2$	$C_{26}H_{17}AsF_{20}O_2$	$C_{30}H_{17}AsF_{28}O_2$
M_w	616.28	816.32	1016.36
cryst syst	orthorhombic	triclinic	triclinic
space group	$P2_12_12_1$	*P*-1	*P*-1
color	colorless	colorless	colorless
habit	plate	plate	plate
a, Å	11.6890(2)	10.5300(2)	10.5400(1)
b, Å	12.0290(2)	11.9040(3)	12.1040(2)
c, Å	16.6230(3)	12.7020(4)	16.1730(3)
α, deg	90	76.8420(10)	81.835(1)
β, deg	90	74.5350(10)	72.973(1)
γ, deg	90	78.0960(10)	66.741(1)
V, Å^3	2337.31(7)	1476.16(7)	1811.70(5)
Z	4	2	2
D_{calcd}, g cm^{-3}	1.751	1.837	1.863
abs. coeff., mm^{-1}	1.569	1.304	1.113
F(000)	1224	804	996
radiation, λ, Å	Mo Kα, 0.71073	Mo Kα, 0.71073	Mo Kα, 0.71073
T, K	173(2)	173(2)	200(2)
data, collected	+*h*, +*k*, +*l*	+*h*, ± *k*, ± *l*	+*h*, ± *k*, ± *l*
data/restraints/params	3129/0/334	6527/0/445	8031/0/553
R_1 [$I > 2\sigma(I)$]	0.0435	0.0509	0.0409
wR_2 (all data)	0.1427	0.1817	0.1378
GOF	1.101	1.194	1.164
CCDC No.	639284	639285	886017

This distinction is a good indication that the steric environment around the arsenic atom of **6b** and **6c** is much more hindered than that of **6a**. In addition, the O-equatorial arsoranes **5** could also be synthesized from the corresponding arsoranides **4-Na**.[67] Since the O-equatorial arsoranes **5** were quantitatively converted into the corresponding O-apical isomers **7** when heated in solution (Scheme 3), the O-equatorial arsoranes were proven to be kinetically stabilized and thermodynamically unstable species. In other words, these are isolable arsoranes with antiapicophilicity which still may undergo stereomutation to their corresponding more stable stereoisomers.

Structure of the Pentacoordinate Arsoranes. Solid-state structures of the O-equatorial spiroarsoranes **5** (**5a**, **5b**, and **5c**) and the O-apical spiroarsoranes **7** (**7a**, **7b**, and **7c**) were confirmed by X-ray crystallographic analysis. ORTEP diagrams for the O-equatorial and O-apical arsoranes are shown in Figure 5. Selected bond lengths and angles are summarized in Table 7. For the O-equatorial isomers, the bond distances of As1−O1 (1.962(2) Å for **5a**, 1.978(2) Å for **5b**, and 1.961(6) Å for **5c**) and As1−C2 (1.978(4) Å for **5a**, 1.986(3) Å for **5b**, and 1.997(9) Å for **5c**) are longer than As1−O2 (1.828(3) Å for **5a**, 1.817(2) Å for **5b**, and 1.827(7) Å for **5c**) and As1−C1 (1.954(4) Å for **5a**, 1.936(3) Å for **5b**, and 1.966(10) Å for **5c**), respectively. This implies that the former two correspond to apical bonds, while the latter two are equatorial bonds, indicating that **5** are essentially of TBP structure. It is noted that the apical bond angles O1−As1−C2 are distorted from the ideal value of 180° with a larger displacement for **5a** (162.07°) than **5b** (164.55°) and **5c** (164.2°). The same goes for the equatorial angle O2−As1−C1 comprising the two bidentates, with that for **5a** (123.86°) being larger than those of **5b** (116.80°) and **5c** (118.6°). Furthermore, the differences between the apical and the equatorial distances for the same atom combinations for **5a** (As−O, 0.13 Å; As−C, 0.02 Å) are smaller than those for **5b** (As−O, 0.16 Å; As−C, 0.05 Å) and **5c** (As−O, 0.14 Å; As−C, 0.03 Å). These structural features indicate that the distortion of **5a** toward the RP (rectangular pyramid) geometry along the Berry coordinate is slightly greater than those of **5b** and **5c**. The lower degree of distortion

dx.doi.org/10.1021/ic3014893 | Inorg. Chem. 2012, 51, 10996−11006

Scheme 1. Synthesis of Tricoordinate Arsine 2

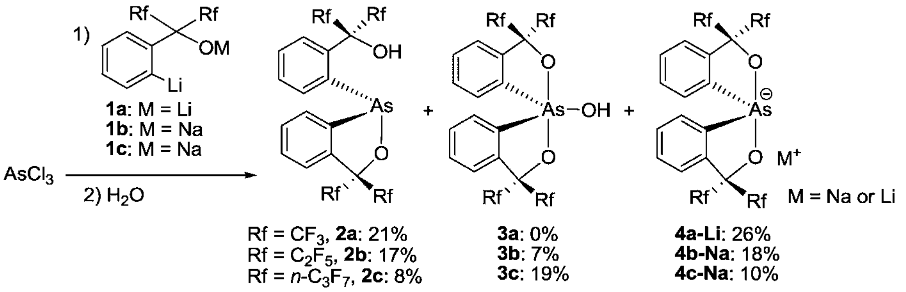

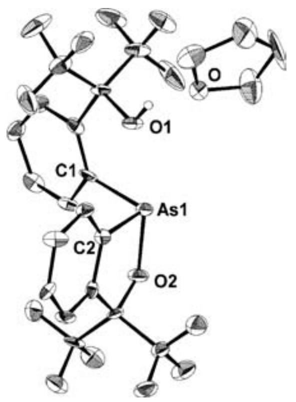

Figure 2. ORTEP diagram of **2a·THF** showing thermal ellipsoids at the 30% probability level. Hydrogen atoms other than that of the hydroxy group are omitted for clarity. Selected bond lengths (Angstroms) and angles (degrees) for **2a**: As1···O1, 2.465; As1–O2, 1.890(15); As1–C1, 2.02(2); As1–C2, 1.91(2); O2–As1–C1, 95.8(9); O2–As1–C2, 85.5(8); C1–As1–C2, 99.1(9).

Table 5. Selected Bond Lengths (Angstroms) and Angles (degrees) for 3a–c

	3a	3b	3c
As1–O1	1.893(2)	1.906(2)	1.905(2)
As1–O2	1.855(2)	1.875(2)	1.874(2)
As1–O3	1.739(2)	1.737(2)	1.743(2)
As1–C1	1.907(3)	1.917(3)	1.912(3)
As1–C2	1.906(3)	1.913(3)	1.912(3)
O1–As1–O2	179.03(9)	179.20(10)	178.12(9)
O1–As1–O3	90.31(11)	91.44(11)	91.69(10)
O1–As1–C1	85.90(12)	85.53(12)	85.68(11)
O1–As1–C2	93.80(12)	92.68(12)	91.85(11)
O2–As1–O3	89.37(11)	88.66(12)	89.53(10)
O2–As1–C1	93.45(12)	95.15(13)	95.14(11)
O2–As1–C2	87.16(12)	86.55(12)	86.34(11)
C1–As1–C2	126.98(13)	131.03(16)	130.83(13)
C1–As1–O3	118.83(12)	114.85(14)	113.42(12)
C2–As1–O3	114.19(12)	114.12(15)	115.74(12)

of **5b** and **5c** could be due to steric repulsion between the two nearest C_2F_5/n-C_3F_7 groups within the molecules. For analogous antiapicophilic phosphoranes with the *t*-Bu group as the monodentate, the structural differences between the CF_3[52] and the C_2F_5[61] compounds were found to be small, with, for instance, the apical bond angle being 169.5(1)° and 169.76(9)° and the angle between the bidentates being 120.7(2)° and 118.02(9)°, respectively, for the former and latter. Thus, the observed distortion in the arsorane system could be due to the larger bidentate ring strain imposed due to the larger atom radius of the arsenic atom. In the O-apical arsoranes **7** (**7a**, **7b**, and **7c**), the apical bond angles O1–As1–O2 (170.82(14)° for **7a**, 166.09(12)° for **7b**, and 166.66(8)° for **7c**) are distorted from the ideal value of 180°, compared with those of **3** with a hydroxyl group as the equatorial monodentate (179.03(9)° for **3a**, 179.20(10)° for **3b**, and 178.12(9)° for **3c**) but to a lesser degree than their

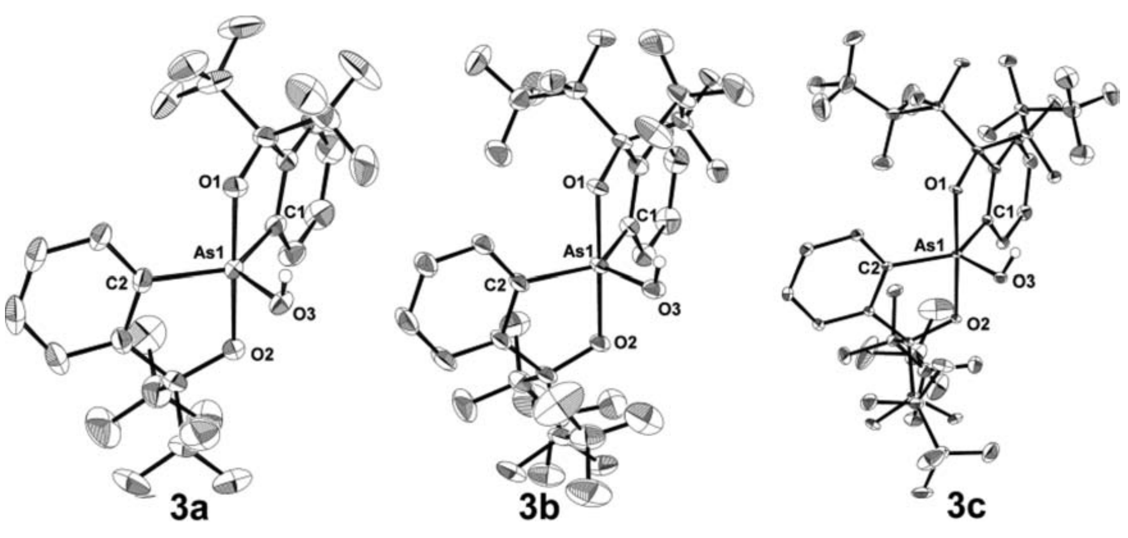

Figure 3. ORTEP diagrams of **3a–c** showing thermal ellipsoids at the 30% probability level. Hydrogen atoms other than that of the hydroxy group are omitted for clarity.

dx.doi.org/10.1021/ic3014893 | *Inorg. Chem.* 2012, 51, 10996–11006

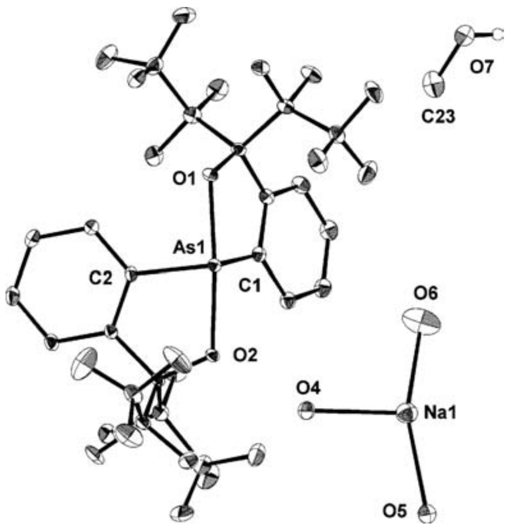

Figure 4. ORTEP diagram of **4b−Na·MeOH·3H$_2$O** showing thermal ellipsoids at the 30% probability level. Hydrogen atoms other than that of the hydroxy group are omitted for clarity.

Table 6. Selected Bond Lengths (Angstroms) and Angles (degrees) for 4b−Na·MeOH·3H$_2$O

	4a−Et$_4$N[75]	4b−Na·MeOH·3H$_2$O
As1−O1	2.011(4)	2.071(2)
As1−O2	2.064(4)	2.053(2)
As1−C1	1.947(6)	1.968(3)
As1−C2	1.975(6)	1.970(3)
O1−As1−O2	169.0(2)	168.39(7)
O1−As1−C1	82.0(2)	81.04(11)
O1−As1−C2	91.8(2)	92.05(10)
O2−As1−C1	91.8(2)	91.81(10)
O2−As1−C2	80.5(2)	81.30(10)
C1−As1−C2	100.9(3)	107.37(11)

corresponding O-equatorial isomers. The C1−As1−C2 angles of **7b** (132.19°) and **7c** (131.19°) are widened by 7° compared with that of **7a** (124.4°), probably due again to the steric differences of the ligands. Notable is that the structural parameters about the central arsenic atom are practically the same between **7b** and **7c**, although the conformations of the fluorinated carbon groups are different. Thus, distinct structural differences were observed between corresponding isomers of the CF_3 and C_2F_5 series, whereas the changes between the C_2F_5 and C_3F_7 derivatives were not as obvious. The structures of iodoarsoranes **6b** and **6c** were confirmed by X-ray crystallography (Figure 6). The equatorial bond lengths of As1−I1 were 2.529(4) Å for **6b** and 2.5090(5) Å for **6c**.[80] The other bonds and angles of the iodoarsoranes were very similar to those of our previously reported O-apical arsoranes.[23]

Scheme 3. Isomerization of O-Equatorial Arsoranes to Their O-Apical Arsoranes

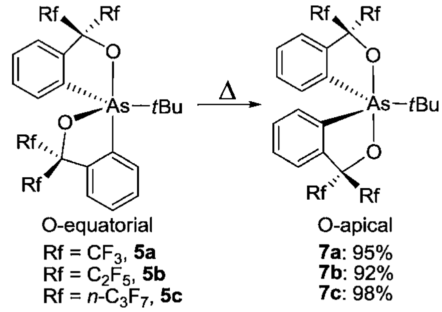

Kinetic Study. Kinetic measurements for isomerization of **5** to **7** were performed in *p-tert*-butyltoluene over the temperature range of 60−80 °C for **5a** to **7a**, 85−105 °C for **5b** to **7b**, and 95−115 °C for **5c** to **7c** by monitoring the change in the integrals of the ^{19}F NMR signals of the trifluoromethyl groups (Table 8). Eyring plots of the rates showed good linearity for all three temperatures (Figure 7). The activation parameters derived from the plots for the CF_3 derivatives (**5a** to **7a**) are $\Delta H^‡ = 26.0 \pm 0.3$ kcal mol^{-1}, $\Delta S^‡ = -2.1 \pm 0.8$ e.u., $\Delta G^‡_{363} = 26.8$ kcal mol^{-1}, those for the C_2F_5 derivatives (**5b** to **7b**) are $\Delta H^‡ = 28.2 \pm 0.7$ kcal mol^{-1}, $\Delta S^‡ = -0.6 \pm 2.0$ e.u., $\Delta G^‡_{363} = 28.4$ kcal mol^{-1}, and those for the *n*-C_3F_7 derivatives (**5c** to **7c**) are $\Delta H^‡ = 28.6 \pm 0.6$ kcal mol^{-1}, $\Delta S^‡ = -0.3 \pm 1.6$ e.u., $\Delta G^‡_{363} = 28.7$ kcal mol^{-1} (Table 8, Figure 7). The activation entropies ($\Delta S^‡$) for all three were about the same with near zero values. The difference in activation free energy for isomerization of **5a** and **5b** was 1.6 (28.4–26.8) kcal mol^{-1}, indicating that increasing steric effects by changing CF_3 to C_2F_5 was highly effective for slowing down BPR. A comparison of the rates of isomerization of **5b** and **5c** at the same temperature (95, 100, and 115 °C) shows that the isomerization rate for **5c** has been reduced to about one-half. Therefore, it could be said that the steric effect of the *n*-C_3F_7 group is unnegligible. This difference in rate corresponds to a difference in activation free energy of 0.3 (28.7 − 28.4) kcal mol^{-1}. Thus, the substituent effect upon changing from C_2F_5 to *n*-C_3F_7 was not as significant as that for the change from CF_3 to C_2F_5. This is understandable by considering the global maximum of the whole stereomutation process, which could be approximated as the highest energy intermediate where one of the bidentates occupies diequatorial sites, as shown in Figure 8.[49,50,52−69] It would be easy to imagine that the terminal CF_3 groups of the C_3F_7

Scheme 2. Synthesis of O-Equatorial Arsoranes

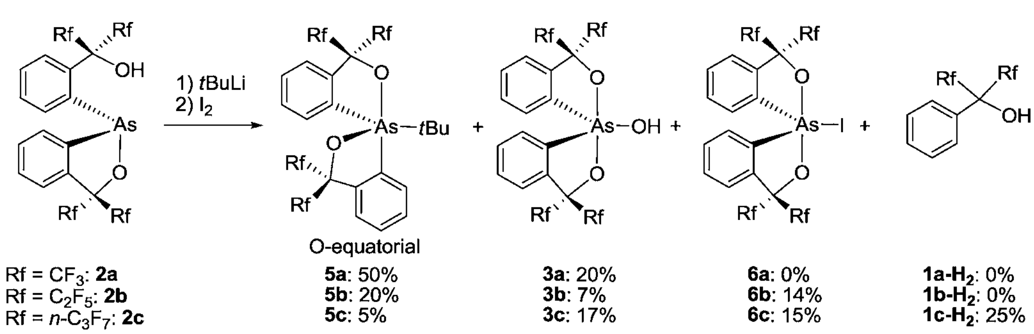

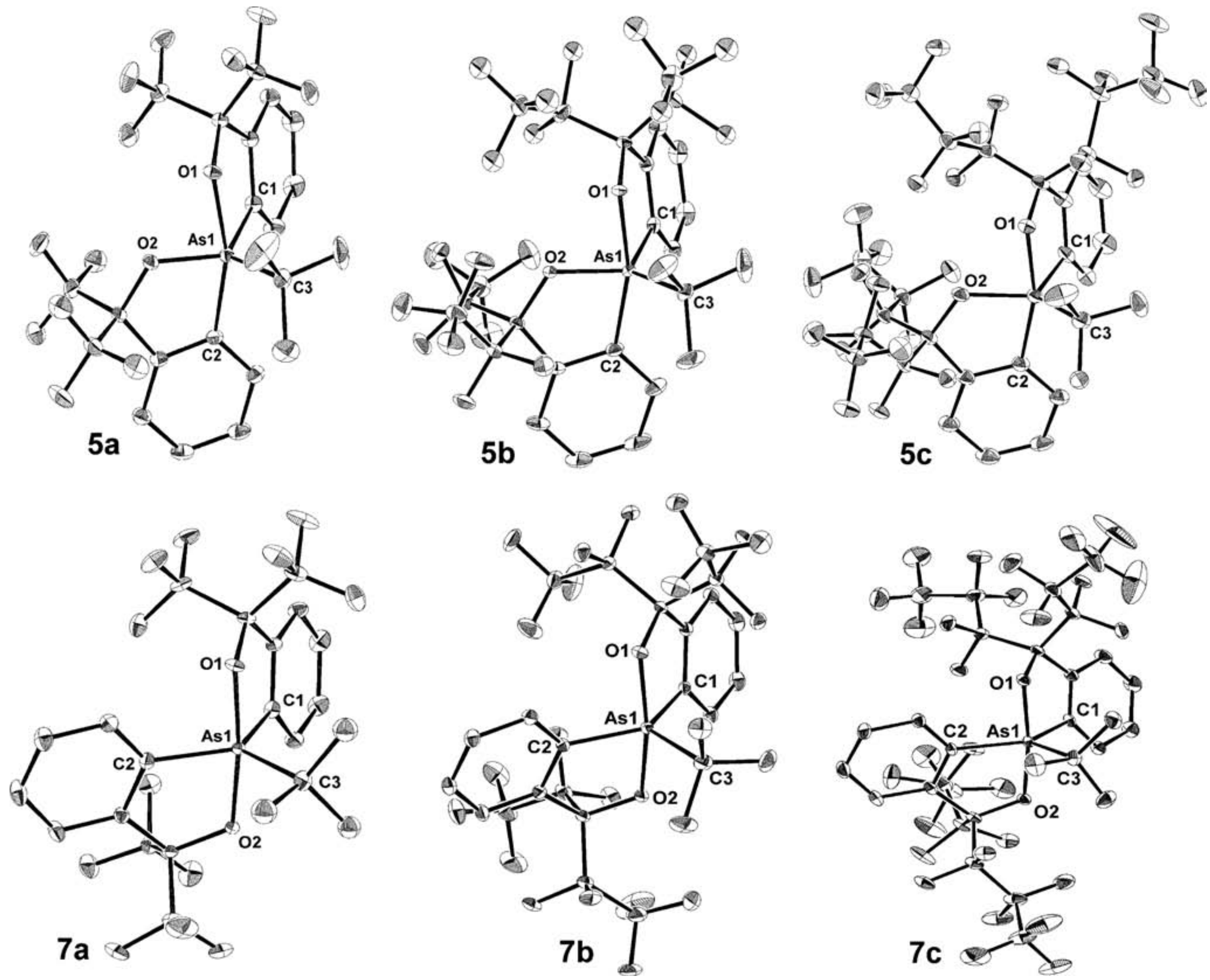

Figure 5. ORTEP diagrams of **5a**–**c** and **7a**–**c** showing thermal ellipsoids at the 30% probability level. Hydrogen atoms are omitted for clarity.

Table 7. Selected Bond Lengths (Angstroms) and Angles (degrees) for 5a–7c

	5a[64]	5b[64]	5c	7a[64]	7b[64]	7c
As1–O1	1.962(2)	1.978(2)	1.961(6)	1.931(3)	1.934(3)	1.9305(18)
As1–O2	1.828(3)	1.817(2)	1.827(7)	1.923(3)	1.937(3)	1.9221(18)
As1–C1	1.954(4)	1.936(3)	1.966(10)	1.938(4)	1.928(4)	1.924(2)
As1–C2	1.978(4)	1.986(3)	1.997(9)	1.934(4)	1.929(4)	1.931(2)
As1–C3	2.006(4)	2.014(3)	2.039(10)	2.005(4)	1.996(4)	1.998(2)
O1–As1–O2	78.59(11)	82.28(10)	80.2(3)	170.82(14)	166.09(12)	166.66(8)
O1–As1–C1	83.02(14)	82.71(12)	83.0(4)	83.82(17)	83.79(14)	83.66(9)
O1–As1–C2	162.07(14)	164.55(13)	164.2(4)	91.42(18)	91.61(14)	91.33(9)
O1–As1–C3	91.46(16)	89.64(13)	89.8(4)	93.45(16)	98.80(16)	95.64(10)
O2–As1–C1	123.86(15)	116.80(12)	118.6(4)	91.66(17)	89.49(14)	90.21(9)
O2–As1–C2	85.15(14)	84.99(13)	84.8(4)	84.53(17)	83.89(14)	83.80(9)
O2–As1–C3	113.55(16)	118.59(14)	117.4(4)	95.72(16)	95.09(16)	97.67(10)
C1–As1–C2	100.13(17)	99.99(15)	100.1(4)	124.4(2)	132.19(16)	131.19(10)
C1–As1–C3	119.53(17)	121.65(15)	121.2(4)	116.96(18)	116.60(18)	113.80(10)
C2–As1–C3	102.02(17)	101.55(15)	101.4(4)	118.58(18)	111.14(19)	115.01(10)

groups are too far away to impose significant steric effects in the vicinity of the central As atom. A comparison with phosphoranes shows that the activation free energies for the arsoranes ($\Delta G^{\ddagger}_{363}$) are much lower than those for the corresponding *t*-Bu-substituted phosphoranes where the activation Gibbs free energy was calculated to be 31.1 kcal mol^{-1} for the CF_3 system[53] and estimated to be ca. 38 kcal mol^{-1} for the C_2F_5 system.[61,64] This is in accordance with the generally easier stereomutation for lower elements in the same group of the periodic table.[69] The differences in activation free

dx.doi.org/10.1021/ic3014893 | *Inorg. Chem.* 2012, 51, 10996−11006

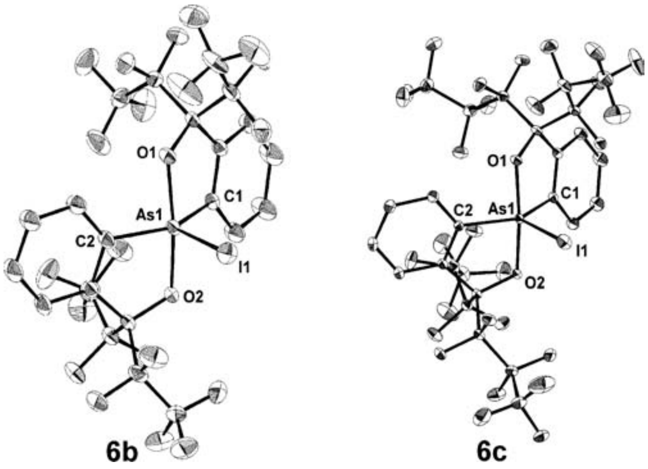

Figure 6. ORTEP diagrams of **6b** and **6c** showing thermal ellipsoids at the 30% probability level. Selected bond lengths (Angstroms) and angles (degrees) for **6b**: As1−O1, 1.891(2); As1−O2, 1.891(2); As1−C1, 1.919(3); As1−C2, 1.919(3); As1−I1, 2.529(4); O1−As1−O2, 168.75(16); O1−As1−C1, 85.41(13); O1−As1−C2, 90.70(13); O1−As1−I1, 95.62(8); O2−As1−C1, 90.70(13); O2−As1−C2, 85.41(13); O2−As1−I1, 95.62(8); C1−As1−C2, 139.5(2); C1−As1−I1, 110.25(12); C2−As1−I1, 110.25(12). Selected bond lengths (Angstroms) and angles (degrees) for **6c**: As1−O1, 1.898(2); As1−O2, 1.898(2); As1−C1, 1.922(3); As1−C2, 1.922(3); As1−I1, 2.5090(5); O1−As1−O2, 170.62(13); O1−As1−C1, 85.50(10); O1−As1−C2, 90.86(10); O1−As1−I1, 94.69(6); O2−As1−C1, 90.86(10); O2−As1−C2, 85.50(10); O2−As1−I1, 94.69(6); C1−As1−C2, 134.29(17); C1−As1−I1, 112.85(8); C2−As1−I1, 112.85(8).

energy between the CF_3 and the C_2F_5 groups, 7 (38 − 31.1) kcal mol^{-1} for the phosphoranes and 1.6 (28.4 − 26.8) kcal mol^{-1} for the arsoranes, indicate that the arsoranes are less prone to steric hindrance.

CONCLUSIONS

In summary, by utilizing bulky bidentate ligand systems with C_2F_5 and n-C_3F_7 groups, new antiapicophilic arsoranes (**5b** and **5c**, respectively) could be synthesized. Both compounds were characterized by X-ray structural analysis. These antiapicophilic arsoranes isomerized to their more stable isomers (**7b** and **7c**, respectively) upon heating, and a kinetic study on this process showed that the barriers increased in the order of $CF_3 < C_2F_5 < n\text{-}C_3F_7$. This proves that increasing steric hindrance is a

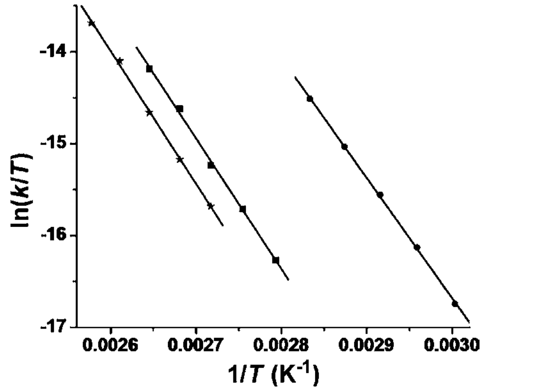

Figure 7. Eyring plot for stereomutation of **5** to **7**: (circle) **5a** to **7a**; (square) **5b** to **7b**; (star) **5c** to **7c**.

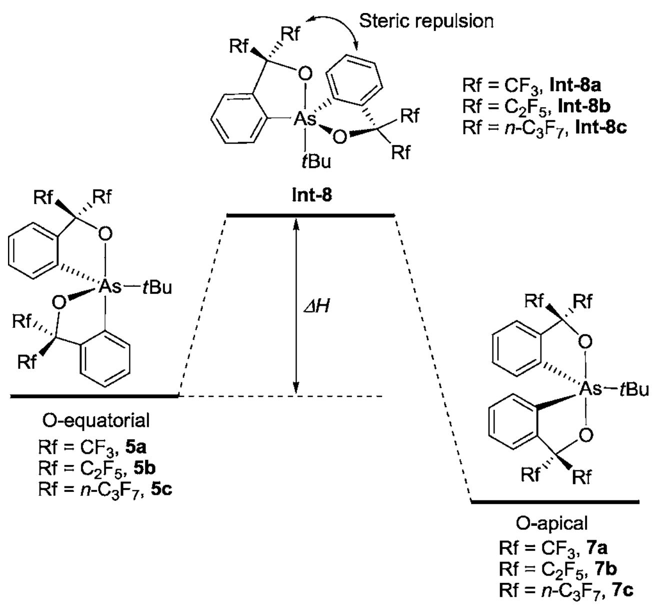

Figure 8. Energy diagram for isomerization of O-equatorial arsoranes to O-apical isomers.

Table 8. Kinetic Parameters[a]

process	T [K]	k [s^{-1}]	$\Delta H^‡$ [kcal mol^{-1}]	$\Delta S^‡$ [e.u.]	$\Delta G^‡_{363}$ [kcal mol^{-1}]
	333	$(1.78 \pm 0.02) \times 10^{-5}$			
	338	$(3.34 \pm 0.01) \times 10^{-5}$			
5a → **7a**	343	$(6.01 \pm 0.02) \times 10^{-5}$	26.0 ± 0.3	−2.1 ± 0.8	26.8
	348	$(10.3 \pm 0.09) \times 10^{-5}$			
	353	$(17.6 \pm 0.20) \times 10^{-5}$			
	358	$(3.08 \pm 0.05) \times 10^{-5}$			
	363	$(5.47 \pm 0.11) \times 10^{-5}$			
5b → **7b**	368	$(8.90 \pm 0.19) \times 10^{-5}$	28.2 ± 0.7	−0.6 ± 2.0	28.4
	373	$(16.7 \pm 0.36) \times 10^{-5}$			
	378	$(26.1 \pm 0.32) \times 10^{-5}$			
	368	$(5.69 \pm 0.15) \times 10^{-5}$			
	373	$(9.61 \pm 0.21) \times 10^{-5}$			
5c → **7c**	378	$(16.2 \pm 0.04) \times 10^{-5}$	28.6 ± 0.6	−0.32 ± 1.56	28.7
	383	$(28.8 \pm 0.06) \times 10^{-5}$			
	388	$(44.1 \pm 0.10) \times 10^{-5}$			

[a]Error is given as the standard deviation.

reasonable way for kinetically stabilizing antiapicophilic arsoranes as in the case of phosphoranes. The change from CF_3 to C_2F_5 led to an increase in the activation free energy at 363 K of 1.6 kcal mol^{-1}, indicating that the change was significant. On the other hand, upon changing from C_2F_5 to *n*-C_3F_7, the difference was reduced to 0.3 kcal mol^{-1}, indicating that although the change is not as potent it is still effective. X-ray structural analysis of several precursors was also carried out, and especially noteworthy is that in arsine **2a**, the interatomic distance between As and O of the hydroxyl group (As1−O1) was 2.465 Å, implying that there is interaction. In addition, rare water-stable iodoarsoranes (**6b** and **6c**) could be fully characterized owing to the steric effect of the C_2F_5 and C_3F_7 groups.

■ ASSOCIATED CONTENT

Ⓢ Supporting Information

X-ray crystallography details and CIF files of compounds **2a·THF**, **3a**, **3b**, **3c**, **4b−Na·MeOH·3H$_2$O**, **5c**, **6b**, **6c**, and **7c**. This material is available free of charge via the Internet at http://pubs.acs.org.

■ AUTHOR INFORMATION

Corresponding Author

*E-mail: xdjiang@henu.edu.cn; yyama@sci.hiroshima-u.ac.jp.

Notes

The authors declare no competing financial interest.

■ ACKNOWLEDGMENTS

The authors are grateful to Central Glass Co., Ltd., for the generous gift of hexafluorocumyl alcohol. This research was supported by the Grant-in-Aid for Scientific Research on Priority Areas (No. 17350021) from the Ministry of Education, Culture, Sports, Science and Technology, Japan and the National Natural Science Foundation of China (20872026).

■ REFERENCES

(1) Akiba, K.-y. *Chemistry of Hypervalent Compounds*; Wiley-VCH: New York, 1999.
(2) Holmes, R. R. Pentacoordinated Phosphorus Structure and Spectroscopy. *ACS Monograph 175*; American Chemical Society: Washington, DC, 1980; Vols. *I* and *II*; p 176.
(3) Corbridge, D. E. C. *Phosphorus: An Outline of Its Chemistry, Biochemistry, and Technology*, 4th ed.; Elsevier: Amsterdam, The Netherlands, 1990; Chapter 14, pp 1233−1256.
(4) Burgada, R.; Setton, R. In *The Chemistry of Organophosphorus Compounds*; Hartley, F. R., Ed.; Wiley-Interscience: Chichester, Great Britain, 1994; Vol. 3, pp 185−277.
(5) Barlett, R. A.; Rasika Dias, H. V.; Flynn, K. M.; Hope, H.; Murray, B. D.; Olmstead, M. M.; Power, P. P. *J. Am. Chem. Soc.* **1987**, *109*, 5693−5698.
(6) Hengge, A. C. *Acc. Chem. Res.* **2002**, *35*, 105−112.
(7) López, C. S.; Faza, O. N.; de Lera, A. R.; York, D. M. *Chem.—Eur. J.* **2005**, *11*, 2081−2093.
(8) Uchimaru, T.; Uebayasi, M.; Hirose, T.; Tsuzuki, S.; Yliniemelä, A.; Tanabe, K.; Taira, K. *J. Org. Chem.* **1996**, *61*, 1599−1608.
(9) Thatcher, G. R. J.; Kluger, R. *Adv. Phys. Org. Chem.* **1989**, *25*, 99−265.
(10) Pavan Kumar, K. V. P.; Satish Kumar, N.; Kumara Swamy, K. C. *New J. Chem.* **2006**, *30*, 717−728.
(11) Holmes, R. R. *Acc. Chem. Res.* **2004**, *37*, 746−753.
(12) Westheimer, F. H. *Acc. Chem. Res.* **1968**, *1*, 70−78.
(13) Martin, J. C. *Science* **1983**, *221*, 509−514.
(14) Kobayashi, J.; Goto, K.; Kawashima, T.; Schmidt, M. W.; Nagase, S. *J. Am. Chem. Soc.* **2002**, *124*, 3703−3712.
(15) Vollbrecht, S.; Vollbrecht, A.; Jeske, J.; Jones, P. G.; Schmutzler, R.; du Mont, W.-W. *Chem. Ber./Recl.* **1997**, *130*, 819−822.
(16) Kumara Swamy, K. C.; Satish Kumar, N. *Acc. Chem. Res.* **2006**, *39*, 324−333.
(17) Bohra, R.; Roesky, H. W. *Adv. Inorg. Radiochem.* **1984**, *28*, 203−254.
(18) Lloyd, D.; Gosney, I.; Ormiston, R. A. *Chem. Soc. Rev.* **1987**, *16*, 45−74.
(19) Gosney, I.; Lillie, T. J.; Lloyd, D. *Angew. Chem., Int. Ed. Engl.* **1977**, *16*, 487−488.
(20) He, S. H.; Chung, C. W. Y.; But, T. Y. S.; Toy, P. H. *Tetrahedron* **2005**, *61*, 1385−1405.
(21) Still, W. C.; Novack, V. J. *J. Am. Chem. Soc.* **1981**, *103*, 1283−1285.
(22) Hsi, J. D.; Koreeda, M. *J. Org. Chem.* **1989**, *54*, 3229−3231.
(23) Jiang, X.-D.; Matsukawa, S.; Fukuzaki, Y.; Yamamoto, Y. *New J. Chem.* **2010**, *34*, 1623−1629.
(24) Betz, R.; Klüfers, P. *Inorg. Chem.* **2009**, *48*, 925−935.
(25) Said, M. A.; Kumara Swamy, K. C.; Veith, M.; Huch, V. *Inorg. Chem.* **1996**, *35*, 6627−6630.
(26) Tapia-Benavides, A. R.; Mendoza-Huizar, L. H.; Pérez-García, F.; Tlahuext, H.; Alvarez, A.; Tlahuextl, M. *Inorg. Chem.* **2010**, *49*, 1496−1502.
(27) Nakamoto, M.; Kojima, S.; Matsukawa, S.; Yamamoto, Y.; Akiba, K.-y. *J. Organomet. Chem.* **2002**, *643−644*, 441−452.
(28) Matsukawa, S.; Kajiyama, K.; Kojima, S.; Furuta, S.-y.; Yamamoto, Y.; Akiba, K.-y. *Angew. Chem., Int. Ed.* **2002**, *41*, 4718−4722.
(29) Trippett, S. *Phosphorus Sulfur Relat. Elem.* **1976**, *1*, 89−98.
(30) Trippett, S. *Pure Appl. Chem.* **1974**, *40*, 595−604.
(31) Buono, G.; Llinas, J. R. *J. Am. Chem. Soc.* **1981**, *103*, 4532−4540.
(32) Eisenhut, M.; Mitchell, H. L.; Traficante, D. D.; Kaufman, R. J.; Deutch, J. M.; Whitesides, G. M. *J. Am. Chem. Soc.* **1974**, *96*, 5385−5397.
(33) Moreland, C. G.; Doak, G. O.; Littlefield, L. B.; Walker, N. S.; Gilje, J. W.; Braun, R. W.; Cowley, A. H. *J. Am. Chem. Soc.* **1976**, *98*, 2161−2165.
(34) Griend, L. V.; Cavell, R. G. *Inorg. Chem.* **1983**, *22*, 1817−1820.
(35) Kumaraswamy, S.; Muthiah, C.; Kumara Swamy, K. C. *J. Am. Chem. Soc.* **2000**, *122*, 964−965.
(36) Kommana, P.; Kumaraswamy, S.; Vittal, J. J.; Kumara Swamy, K. C. *Inorg. Chem.* **2002**, *41*, 2356−2363.
(37) Kommana, P.; Satish Kumar, N.; Vittal, J. J.; Jayasree, E. G.; Jemmis, E. D.; Kumara Swamy, K. C. *Org. Lett.* **2004**, *6*, 145−148.
(38) Hoffmann, R.; Howell, J. M.; Muetterties, E. L. *J. Am. Chem. Soc.* **1972**, *94*, 3047−3058.
(39) McDowell, R. S.; Streitwieser, A., Jr. *J. Am. Chem. Soc.* **1985**, *107*, 5849−5855.
(40) Deiters, J. A.; Holmes, R. R.; Holmes, J. M. *J. Am. Chem. Soc.* **1988**, *110*, 7672−7681.
(41) Wang, P.; Zhang, Y.; Glaser, R.; Reed, A. E.; Schleyer, P. v. R.; Streitwieser, A., Jr. *J. Am. Chem. Soc.* **1991**, *113*, 55−64.
(42) Wasada, H.; Hirao, K. *J. Am. Chem. Soc.* **1992**, *114*, 16−27.
(43) Thatcher, G. R. J.; Campbell, A. S. *J. Org. Chem.* **1993**, *58*, 2272−2281.
(44) Wang, P.; Zhang, Y.; Glaser, R.; Streitwieser, A.; Schleyer, P. v. R. *J. Comput. Chem.* **1993**, *14*, 522−529.
(45) Wladkowski, B. D.; Krauss, M.; Stevens, W. J. *J. Phys. Chem.* **1995**, *99*, 4490−4500.
(46) Berry, R. S. *J. Chem. Phys.* **1960**, *32*, 933−938.
(47) Ugi, I.; Marquarding, D.; Klusacek, H.; Gillespie, P.; Ramirez, F. *Acc. Chem. Res.* **1971**, *4*, 288−296.
(48) Gillespie, P.; Hoffman, P.; Klusacek, H.; Marquarding, D.; Pfohl, S.; Ramirez, F.; Tsolis, E. A.; Ugi, I. *Angew. Chem., Int. Ed. Engl.* **1971**, *10*, 687−715.
(49) Yamamichi, H.; Matsukawa, S.; Kojima, S.; Ando, K.; Yamamoto, Y. *Heteroat. Chem.* **2011**, *22*, 553−561.
(50) Matsukawa, S.; Yamamichi, H.; Yamamoto, Y.; Ando, K. *J. Am. Chem. Soc.* **2009**, *131*, 3418−3419.

(51) Couzijn, E. P. A.; Slootweg, J. C.; Ehlers, A. W.; Lammertsma, K. *J. Am. Chem. Soc.* **2010**, *132*, 18127−18140.
(52) Kojima, S.; Kajiyama, K.; Nakamoto, M.; Akiba, K.-y. *J. Am. Chem. Soc.* **1996**, *118*, 12866−12867.
(53) Kojima, S.; Kajiyama, K.; Nakamoto, M.; Matsukawa, S.; Akiba, K.-y. *Eur. J. Org. Chem.* **2006**, 218−234.
(54) Kajiyama, K.; Yoshimune, M.; Nakamoto, M.; Matsukawa, S.; Kojima, S.; Akiba, K.-y. *Org. Lett.* **2001**, *3*, 1873−1875.
(55) Kojima, S.; Sugino, M.; Matsukawa, S.; Nakamoto, M.; Akiba, K.-y. *J. Am. Chem. Soc.* **2002**, *124*, 7674−7675.
(56) Kojima, S.; Nakamoto, M.; Akiba, K.-y. *Eur. J. Org. Chem.* **2008**, 1715−1722.
(57) Matsukawa, S.; Kojima, S.; Kajiyama, K.; Yamamoto, Y.; Akiba, K.-y.; Re, S.; Nagase, S. *J. Am. Chem. Soc.* **2002**, *124*, 13154−13170.
(58) Adachi, T.; Matsukawa, S.; Nakamoto, M.; Kajiyama, K.; Kojima, S.; Yamamoto, Y.; Akiba, K.-y.; Re, S.; Nagase, S. *Inorg. Chem.* **2006**, *45*, 7269−7277.
(59) Kojima, S.; Nakamoto, M.; Matsukawa, S.; Akiba, K.-y. *Heteroat. Chem.* **2011**, *22*, 491−499.
(60) Yamamoto, Y.; Nakao, K.; Hashimoto, T.; Matsukawa, S.; Suzukawa, N.; Kojima, S.; Akiba, K.-y. *Heteroat. Chem.* **2011**, *22*, 523−530.
(61) Jiang, X.-D.; Kakuda, K.-i.; Matsukawa, S.; Yamamichi, H.; Kojima, S.; Yamamoto, Y. *Chem. Asian J.* **2007**, *2*, 314−323.
(62) Jiang, X.-D.; Matsukawa, S.; Yamamichi, H.; Yamamoto, Y. *Heterocycles* **2007**, *73*, 805−824.
(63) Jiang, X.-D.; Matsukawa, S.; Yamamoto, Y. *Dalton Trans.* **2008**, *28*, 3678−3687.
(64) For preliminary results see: Jiang, X.-D.; Matsukawa, S.; Yamamichi, H.; Yamamoto, Y. *Inorg. Chem.* **2007**, *46*, 5480−5482.
(65) Jiang, X.-D.; Matsukawa, S.; Yamamichi, H.; Kakuda, K.-i.; Kojima, S.; Yamamoto, Y. *Eur. J. Org. Chem.* **2008**, 1392−1405.
(66) Akiba, K.-y.; Nakata, H.; Yamamoto, Y.; Kojima, S. *Chem. Lett.* **1992**, 1559−1562.
(67) Jiang, X.-D.; Yamamoto, Y. *J. Organomet. Chem.* **2010**, *695*, 740−746.
(68) Jiang, X.-D.; Matsukawa, S.; Kakuda, K.-i.; Fukuzaki, Y.; Zhao, W.; Li, L.; Shen, H.; Kojima, S.; Yamamoto, Y. *Dalton Trans.* **2010**, *39*, 9823−9829.
(69) Akiba, K.-y.; Yamamoto, Y. In *The Chemistry of Organic Arsenic, Antimony, and Bismuth Compounds*; Patai, S., Ed.; John Wiley & Sons: Chichester, 1994; p 761 and references therein.
(70) Moreland, C. G.; Doak, G. O.; Littlefield, L. B. *J. Am. Chem. Soc.* **1973**, *95*, 255−256.
(71) Littlefield, L. B.; Doak, G. O. *J. Am. Chem. Soc.* **1976**, *98*, 7881−7882.
(72) Moc, J.; Morokuma, K. *J. Mol. Struct.* **1997**, *436−437*, 401−418.
(73) Otwinowski, Z.; Minor, W. *Methods Enzymol.* **1997**, *276*, 307−326.
(74) Sheldrick, G. M. *Acta Cryst.* **2008**, *A64*, 112−122.
(75) Yamamoto, Y.; Toyota, K.; Wakisaka, Y.; Akiba, K.-y. *Heteroat. Chem.* **2000**, *11*, 42−47.
(76) Granoth, I.; Martin, J. C. *J. Am. Chem. Soc.* **1979**, *101*, 4623−4626.
(77) Chopra, S. K.; Martin, J. C. *Heteroat. Chem.* **1991**, *2*, 71−79.
(78) Bondi, A. *J. Phys. Chem.* **1964**, *68*, 441−451.
(79) The D angle is defined as the difference between the two largest angles around the central atom of a pentacoordinate compound, and species with $D \leq 15°$ are classified as having square pyramidal structure and those with $D \geq 45°$ as having trigonal bipyramidal stucture. For the D angle, see: (a) Schmuck, A.; Leopold, D.; Seppelt, K. *Chem. Ber.* **1989**, *122*, 803−808. (b) Schmuck, A.; Pyykkö, P.; Seppelt, K. *Angew. Chem.* **1990**, *102*, 211−213; *Angew. Chem., Int. Ed. Engl.* **1990**, *29*, 213−215.
(80) Kojima, S.; Takagi, R.; Nakata, H.; Yamamoto, Y.; Akiba, K.-y. *Chem. Lett.* **1995**, 857−858.